# Amplification of the luminescence response in organic materials exposed to ionizing radiation

Maugan Michel, Licinio Rocha, Matthieu Hamel, Stéphane Normand

# Amplification of the Luminescence Response in Organic Materials Exposed to Ionizing Radiation

Maugan Michel, Licinio Rocha, Matthieu Hamel and Stéphane Normand

***Abstract*—Polymer-based scintillators present interesting features for the field of ionizing radiation detection, related to the high sensitivity of fluorescence techniques coupled to the manufacturing advantages of such materials. Organic materials can indeed be manufactured into large sensing areas with different geometrical conformations through low-cost fabrication techniques. While results herein presented focus on liquids, the same phenomena would occur in solid samples.**

**Widely used for sensing applications because of its high sensitivity, fluorescence has yet been further improved using technologies yielded by research in photonics. It has already been shown that the use of nanostructuration for sensing applications enables previously unattained sensitivities.**

**Herein we propose a technique based on the manipulation of light using nanostructuration of the detection medium in order to enable the amplification of the sensitive material emission. This amplification of the luminescence signal is aimed at reducing the detection limit of low-energy beta emitters such as tritium, well-known issue of major importance.**

**The first step of our study, presented here, consists in demonstrating the ability of well-known scintillators to emit in laser regime when optically excited in a Distributed Feedback scheme. They are, to our knowledge, *the first of their kind*.**

**The technique here presented, being usable whatever the sample maximum emission wavelength, should also enable a simplification of the devices based on scintillators.**

***Index Terms*—Laser, Distributed feedback devices, Ionizing radiation sensors, Alpha particles, Beta rays Solid scintillation detectors, Organic materials, Nuclear measurements, Holographic optical components, Kerr effect,**

## NOMENCLATURE

| | |
|---|---|
| Bis MSB | 1,1'-[1,4-Phenylenedi(E)-2,1-ethenediyl]bis(2-methylbenzene). |
| C515 | Coumarin 515: 7-(Diethylamino)-3-(1-methyl-1H-benzimidazol-2-yl)-2H-chromen-2-one. |
| C151 | Coumarin 151: 7-Amino-4-(trifluoromethyl)-2H-chromen-2-one. |
| DIPN | 2,6-Diisopropylnaphthalene. |
| DMSO | Dimethylsulfoxide: (Methylsulfinyl)methane |
| Eto-Napht | N-(2',5'-di-t-butylphenyl)-4-ethoxy-1,8-naphtalimide. |
| PPO | 2,5-Diphenyloxazol. |
| PVK | Poly(vinylcarbazole). |
| Rh6G | Rhodamine 6G: ethyl 2-[(6Z)-3-ethylamino-6-ethylimino-2,7-dimethyl-xanthen-9-yl]benzoate hydrochloride |
| UGAB | Ultima Gold™ AB (PerkinElmer). |

Corresponding author. Tel: +33 1 69 08 25 27, E-mail address: maugan.michel@cea.fr (M. Michel)

Manuscript received November 15, 2012.

M. Michel is with CEA, LIST, Laboratoire Capteurs et Architectures Électroniques, F-91191 Gif-sur-Yvette, France. Telephone: 33 1 69 08 25 27, e-mail: maugan.michel@cea.fr).

L. Rocha, M. Hamel and S. Normand are with the CEA, LIST, Laboratoire Capteurs et Architectures Électroniques, F-91191 Gif-sur-Yvette, France. E-mail: licinio.rocha@cea.fr, stephane.normand@cea.fr

## I. INTRODUCTION

CONTROLLING light in dielectric materials is an important field of photonics. Widely studied for communication technologies, nano-modification of the material properties have found applications in fields ranging from lab-on-chip devices [1] to Martian exobiology [2].

Inducing a periodic variation in a dielectric material's properties in the optical wavelength scale can modify the material's behaviour towards light. Thus inducing gain, refractive index, or topology gratings can change the generation, absorption and propagation of light in the modulated medium. Following diffraction of light propagating in periodic media, privileged light channels can for example be defined. Combined with a primary light amplification phenomenon, in specific structures, great amplification can occur. Interaction of light with nanostructured media can thus be implemented to design devices that are highly sensitive to any modification of the environment, with strong potential for detecting devices [3], [4].

## II. CONTROLLING LIGHT THROUGH NANOSCALE STRUCTURATION – LASER EMISSION IN SCINTILLATORS

Population inversion, required for light amplification by emission of stimulated radiation [5] can be produced in conjugated molecules, through their $\pi$-delocalized electrons. Scintillators, containing such molecules could thus be used as lasing medium.

Appart from the cost reduction due to the use of organic compounds, these materials come with various permanent nanostructuration techniques, also cost effective (see [6] for a review of soft lithography techniques).

The device used in this present study, seen in Fig. 1, generates transient gratings enabling real-time control of the periodic structures characteristics. The gratings are generated by exposing the sample to the interference pattern produced by the superimposition of two excitation laser beams.

The Kerr effect is a non-linear optical effect taking place when a dielectric medium is exposed to a high-intensity optical field $|E_\omega|^2$, leading to a change of the refractive index $n$, as shown by Eq. (1):

$$n(E) = n_0 + \frac{3\chi^{(3)}}{8n_0}|E_\omega|^2 = n_0 + \Delta n \qquad (1)$$

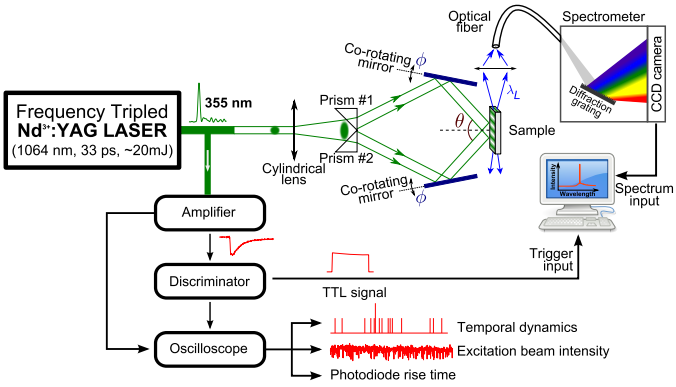


Fig. 1. Schematic of the dynamic Distributed Feedback grating experimental setup. The interference pattern creates gain and refractive index gratings. Prisms are UV-grade silica. Corotation angle of the mirrors is controlled through a linear translation stage.
Materials are excited with the second (532 nm) or third (355 nm) harmonics of a picosecond $Nd^{3+}$:YAG laser.

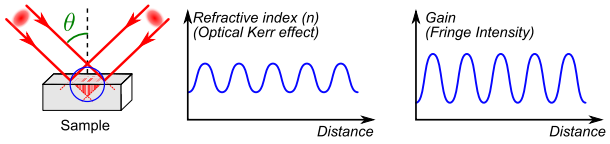


Fig. 2. Index and gain gratings created by the interference pattern of two coherent beams in a material.

Where $n_0$ is the linear refractive index, $\chi^{(3)}$ the third-order susceptibility of the material and $\Delta n$ the refractive index variation induced by light.

This gives an intensity-dependent refractive index, which would vary periodically according to the intensity modulation of an interference pattern, achieved by interfering two coherent beams.

The experimental setup for such transient grating is presented in Fig. 1. The intensity of the fringes defines the amplitude of the grating. The spacing of the fringes, depending on the interfering angle $\theta$ of the two coherent beams of exc wavelength, controlled by the corotating mirrors, defines the grating's period $\Lambda$; it is calculated using Eq. (2):

$$\Lambda = \frac{\lambda_{\text{exc}}}{2\sin\theta} \tag{2}$$

As well as a refractive index grating, a gain grating is also created thanks to the periodic illuminance (see Fig. 2).

The diffraction of light in particular gratings can produce Distributed Feedback (DFB) in which the diffracted beam contra-propagates in the grating, exchanging energy with the propagating wave all along the grating [7]. Provided sufficient gain and excitation, the ensuing resonant structure provides an amplification in the material resulting in a Distributed Feedback laser emission (see Fig. 3). The emitted wavelength $\lambda_{\text{em}}$ for this lasing condition to be verified, called the Bragg condition, is calculated using Eq. (3):

$$\lambda_{\text{Bragg}} = \lambda_{\text{em}} = \frac{2n_{\text{eff}}\Lambda}{p} \tag{3}$$

Where $n_{\text{eff}}$ the effective refractive index of the medium where the grating exists, $p$ the diffraction order.

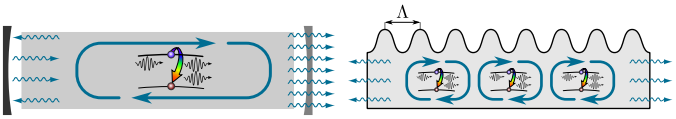


Fig. 3. Conventional (left) and Distributed Feedback (right) lasers feedback schemes. While feedback in the gain medium (undergoing stimulated emission) in conventional lasers is provided by the mirrors, in a Distributed Feedback scheme, it occurs all along the grating.

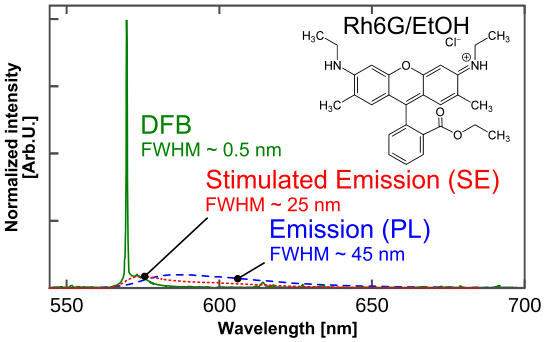


Fig. 4. Fluorescence (dashed line), Stimulated Emission (short dashed line) and Distributed Feedback (continuous line) spectra and structure of Rhodamine 6G in Ethanol ($5 \cdot 10^{-3}$ mol/L). Fluorescence spectrum was measured using a Fluoromax4 spectrofluorometer (HORIBA), $\lambda_{\text{exc}} = 357$ nm; DFB spectrum measured using a Multispec spectrometer (Oriel), coupled to a DV401-SI (Andor Technology) camera.
DFB excitation beam: frequency doubled (532 nm) pulsed picosecond $Nd^{3+}$:YAG laser.

$\lambda_{\text{Bragg}}$ in Eq. (3) is the Bragg wavelength. When dealing with a pure refractive index grating, an even number of peaks will appear centered on this wavelength and separated by a $n_1 c/\lambda$ frequency gap, where $n_1$ is the gain modulation amplitude. Since pure gain or refractive index gratings cannot be achieved under our current experimental configuration, it is a competition between them that is observed.

It appears from Eq. (2) that the emission wavelength is directly related to the beams intersection angle. Thus, changing the angle of the corotating mirrors enables continuous tuning of the emitted photon wavelength. Since there is a feedback between the light-induced optical properties and the resulting emitted light propagation properties, it can be said that light can interact with light and thus can control it [8].

The experimental setup (Fig. 1) used to generate the interference pattern, needed for the transient gratings creation, uses a 20 mJ pulsed picosecond $Nd^{3+}$:YAG laser. Initially emitting a 1064 nm beam, excitation wavelengths of 532 nm and 355 nm can be obtained by frequency conversion, using non-linear optical crystals (in this case, potassium dihydrogen phosphate, KDP). The doubling or tripling of the frequency is chosen based on the absorption properties of the sample.

As a preleminary study, Rhodamine 6G (Rh6G), a widely investigated laser dye has been used in order to calibrate the device. Fig. 4 shows the molecular structure of the Rh6G laser dye, as well as its emission (photoluminescence) and a typical emission spectrum once the DFB conditions are verified (laser excitation beam frequency is here doubled). The laser peak typically is one to two orders of magnitude more intense than the *stimulated emission* maximum. Its full-width at half-

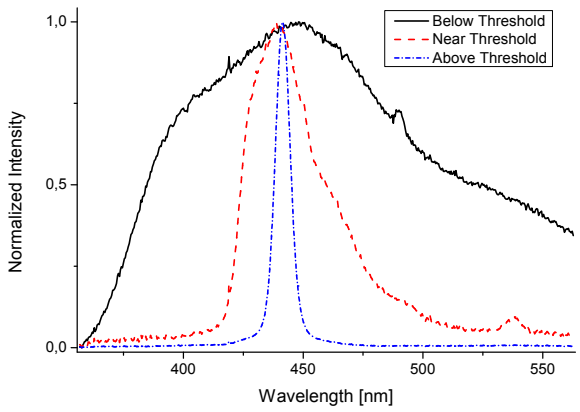


Fig. 5. Spectra showing the linewidth change between above and below stimulated emission threshold for Eljen's EJ200 plastic scintillator. Excitation beam: tripled (355 nm) pulsed picosecond $Nd^{3+}$:YAG laser.

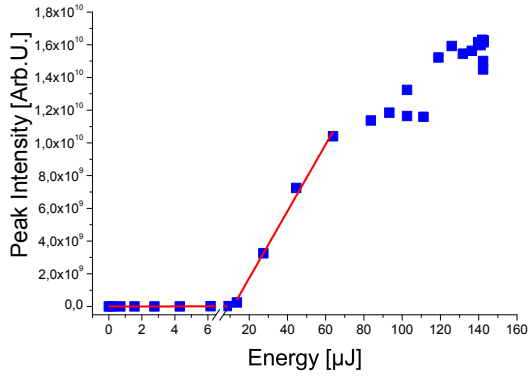


Fig. 6. Eljen's EJ200 plastic scintillator output power *vs* incident pump *energy* plot. Excitation power is then calculated by using the excited zone's cross-section. Excitation beam: tripled (355 nm) pulsed picosecond $Nd^{3+}$:YAG laser. The vertically focalised beam has an estimated maximum energy density of 250 mJ/cm$^2$.

maximum is approximately 0.5 nm.

## III. Candidate Samples Study

### A. Stimulated Emission Threshold Determination

In order to achieve lasing and furthermore DFB lasing, one first has to reach the stimulated emission threshold. This threshold can clearly be seen when increasing the excitation intensity density of a sample while monitoring both linewidth and light output power. Figs. 5 and 6 show Eljen's EJ-200 [1] plastic scintillator spectra and light output intensity at different excitation intensities where the linearity break corresponding to the stimulated emission threshold crossing is evidenced. Both linearity break and changing linewidth have to be verified to qualify for stimulated emission [10].

The control of the incident beam energy per pulse is achieved with a homemade variable attenuator. Shown in Fig. 7, it is based on a rotating half-wavelength plate (HWP) combined with a linear polarizer. Controlling the half-wavelength plate's angle rotates the polarization vector

[1]Commercial equivalents to EJ-200 : Saint Gobain BC-408 and NE Pilot F [9].

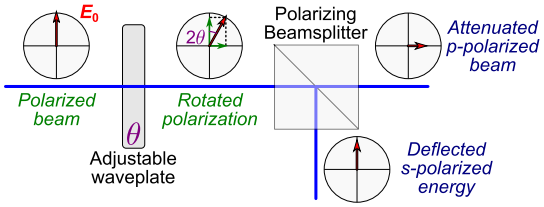


Fig. 7. Homemade variable attenuator principle. Controlling the phase-shift by using a half-wavelength plate enables to continuously control the outgoing linearly polarized beam intensity.

of the linearly polarized incident beam. The beam is then transmitted according to a chosen polarization by an optical linear polarizer.

The key property to qualify an emission for (DFB) lasing is the strong influence of the resonator. This influence is easily demonstrated when DFB lasing is occuring because the lasing peak wavelength depends on the periodicity of the grating which acts as the resonator. Since tuning the period of the grating, rendered easy when working with dynamic gratings as we do, should change the emission wavelength. If this behaviour is demontrated, along with an emitted energy redistribution in the selected peak, it can be asserted DFB lasing is occuring.

The following samples have been tested as concerns the possibility to induce stimulated emission:

- BC-501A (Saint Gobain Crystals),
- Ultima Gold™ AB (Perkin Elmer),
- Two homemade liquid scinitllators based on the Ultima Gold™ AB available composition information [11]. Solvant and primary solute for both samples are DIPN and PPO at 2.5%wt, respectively. Concentration of the secondary solute, Bis MSB is:
  - 0.1%wt in UGAB'-1,
  - 0.2%wt in UGAB'-2
- EJ-200 $10 \times 10 \times 50$ mm bar plastic scintillator,
- Coumarin 151 spin-coated films of a $10^{-2}$mol/L and $2 \cdot 10^{-2}$mol/L concentration in Poly(vinylcarbazole) (PVK) on a microscope plate,
- Eto-Napht [12] in toluene ($10^{-2}$mol/L ),

All liquid samples are contained in spectroscopy-grade quartz (QS) cuvettes of 1 mm, 2 mm or 10 mm optical path.

From the measured stimulated emission thresholds values (see Tab. I), only Eto-Napht cannot be used as a medium for DFB lasing.

### B. Scintillating Ability

Completing the previous study, another test was set-up to verify the ability of some candidates to scintillate. Exposed to, either an alpha radioactive source for solid samples ($^{241}$Am, 21.5 kBq), or a beta radioactive source for liquid samples ($^{90}$Sr/$^{90}$Y, 25 MBq). Measurement was undertaken using a H10720-01 Hamamatsu photomultiplier hermetically sealed from light and coupled to a classic gamma spectroscopy chain. Data were vizualized using Ortec's MAESTRO. Qualitative results are compiled in Tab. I.

TABLE I
STIMULATED EMISSION THRESHOLD OF POTENTIAL CANDIDATE COMPOUNDS TO TRANSDUCING MATERIAL.

| Sample | Stimulated Emission Threshold (mJ/cm$^2$) | Scintillates? |
|---|---|---|
| **EJ-200** | 0.35 | yes |
| **BC-501A** | 0.078 | yes |
| **Ultima Gold$^{TM}$ AB** | 0.043 | yes |
| **UGAB'-1** | 0.026 | yes |
| **UGAB'-2** | 0.039 | yes |
| **Rh6G+Ethanol** | N/A | no |
| **Rh6G+DMSO** | N/A | no |
| **Eto-Napht+Toluene** | $> 250$ | no |

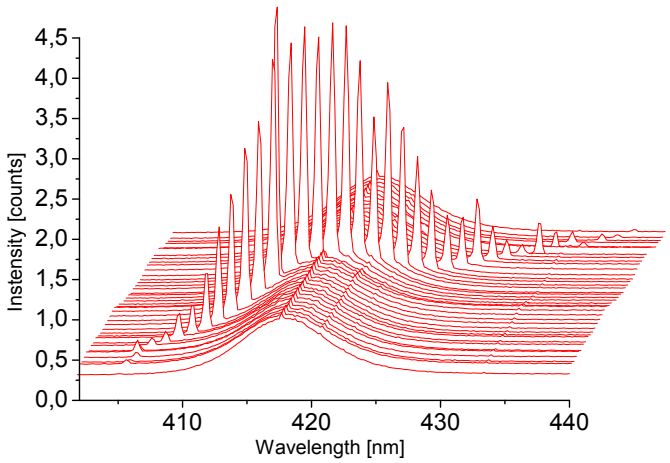


Fig. 8. Variation of the DFB peak wavelength with corotation linear stage position for Ultima Gold$^{TM}$ AB. The interfering angle is directly linked to the the position of the linear translation stage (coupled to both mirror axes). The decrease in peak intensity circa 428 nm is due to non-optimized structuration. DFB excitation beam: tripled (355 nm) pulsed picosecond Nd$^{3+}$:YAG laser.

Although standard laser dyes and solvents (Rh6G in ethanol, Rh6G in DMSO) have been tested for their good lasing properties, no scintillation has been observed, explained by the non-fluorescent matrices which cannot transfer absorbed energy to the dye.

## IV. Distributed Feedback Lasing of Commercial Liquid Scintillators

The samples that have been studied are Ultima Gold$^{TM}$ AB (UGAB) and NE-213/BC-501A (Saint-Gobain Crystals), both widely used commercial liquid scintillators. Considering their absorption spectra, excitation is provided by frequency-tripling the Nd$^{3+}$:YAG laser ($\lambda = 355$ nm).

As can be seen from Figs. 8 and 9, although not designed for this purpose, we report Distributed Feedback (DFB) lasing for both samples. The tuning of the DFB laser wavelength of UGAB ranges over 30 nm (405 – 438 nm). Also clearly appears the important amplification due to DFB. The ratio between DFB and stimulated emission peaks intensities, $\frac{\text{DFB}}{\text{SE}}$ is a good indicator of this amplification; values of 24 and 65 for UGAB and BC-501A respectively have been reached.

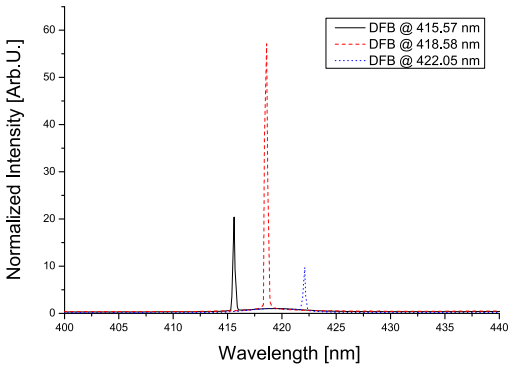


Fig. 9. Variation of the DFB peak wavelength with corotation linear stage position for BC-501A. Stimulated Emission intensity is the normalization factor. DFB excitation beam: tripled (355 nm) pulsed picosecond Nd$^{3+}$:YAG laser.

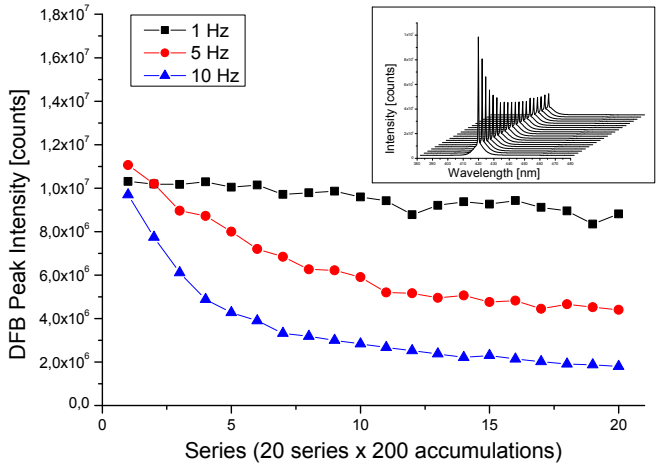


Fig. 10. DFB peak intensity decrease of an Ultima Gold$^{TM}$ AB sample *vs.* excitation repetition rate at a constant incident beam energy.
Inset: successively measured DFB laser spectra at a 10 Hz repetition rate. Due to intrinsic incident beam instability and in order to smooth out the measurements, each plotted spectrum (series) is the accumulation of 20 measured spectra.

### *A. Stability of the DFB Laser Emission vs. Excitation Repetition Rate and Incident Beam Power*

In addition to determining the stimulated emission thresholds of our samples, the continous attenuator is used to set the excitation power so as to lessen sample damaging over time. Laser, and furhermore UV-laser irradiation, irreversibly lowers solid samples lasing abilities due to photobleaching and permanent etching of the material.

This phenomenon has been observed in liquid samples such as UGAB, as shown in Fig. 10. In the case where degradation worsens with higher repetition rate it is assumed that UGAB's viscosity is too high to allow the laser-irradiated sample volume to be sufficiently renewed between each excitation. The same tendency has been observed with variation of the beam intensity: higher beam intensities leading, as expected, to faster degradation of the luminescence properties (see Fig. 11).

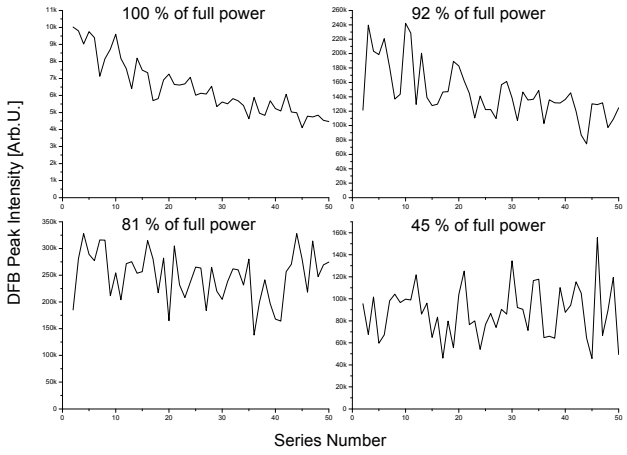


Fig. 11. DFB peak intensity decrease of an Ultima Gold™ AB sample over time *vs.* incident beam power at a 5 Hz excitation repetition rate.

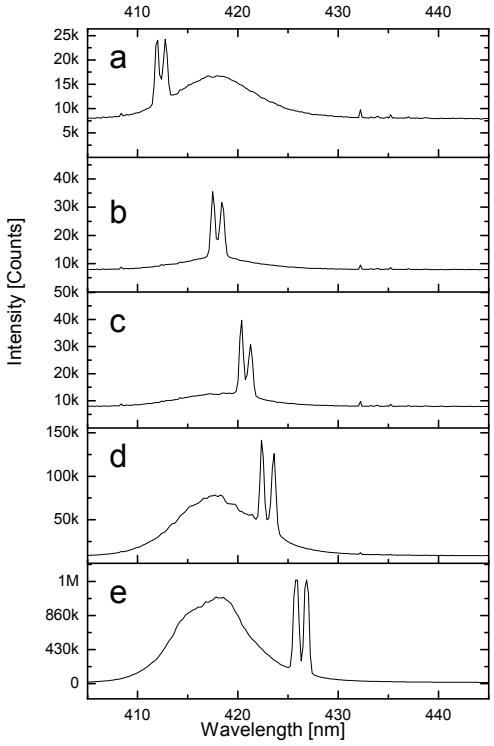


Fig. 12. DFB peaks splitting, showing the coexistence of refractive index and gain gratings.

### *B. Multiple DFB Peaks and Remanent Nanostructure*

Another phenomenon observed when increasing excitation energy is the previously discussed competition between gain and refractive index gratings. The presence of the index grating as revealed by the mode splitting observed in Fig. 12. This mode splitting corresponds to the induction of a band gap as described by the theory of propagating waves in periodic media by Kogelnik and Shank [13].

Presented in Fig. 13, it has also been observed while tuning the dynamic grating period: as a pair of peaks moved to lower wavelengths, a pair of peaks still existed where the dynamic

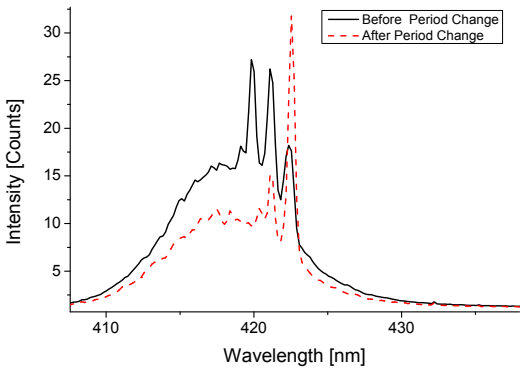


Fig. 13. Coexistence of semi-permanent and dynamic gratings after changing dynamic grating's period. The period changed occured after a long excitation time and high input power. The semi-permanent grating disappeared shortly after the measurement was taken.

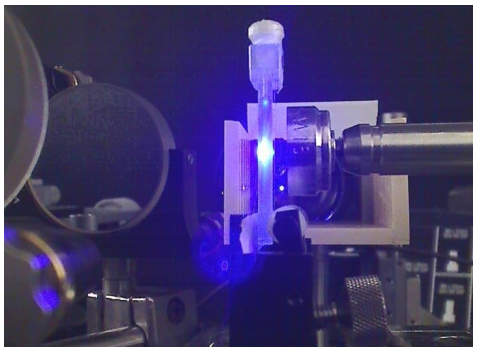

Fig. 14. Picture of an UGAB sample under both laser (bright spot) and ionizing radiation exposure. From left to right: corotating mirrors, Ultima Gold™ AB in a 1 mm quartz and a 25 MBq $^{90}$Sr/$^{90}$Y radioactive source.

peaks previously existed. The high viscosity of UGAB is probably responsible for the existence of this remanent grating as low molecule mobility slows down material homogenization.

### *C. DFB Lasing Under Ionizing Radiation Exposure*

In order to observe the effect of ionizing radiation on the DFB laser, a beta $^{90}$Sr/$^{90}$Y radioactive source was held the nearest from the sample as possible (see Fig. 14). The source is then taken out and put back in the exact same place *via* a mechanical apparatus.

No wavelength shift is observed and, as seen in Fig. 15, no DFB peak intensity variation is observed when source is in place (source ON) or not (source OFF).

## V. Discussion

Dynamic DFB lasing in UGAB does not experience significant wavelength or intensity change when exposed to $\beta$ rays from a 25 MBq $^{90}$Sr/$^{90}$Y radioactive source.

The lack of variation in laser emission was not expected since with the experimental configuration chosen here, an estimated deposited particle energy of a few microjoules is expected.

A first hypothesis would involve energy transfer processes in the scintillator, modified by the excitation energy of the laser (see Fig. 16). In the case of UGAB, assumed to be a ternary

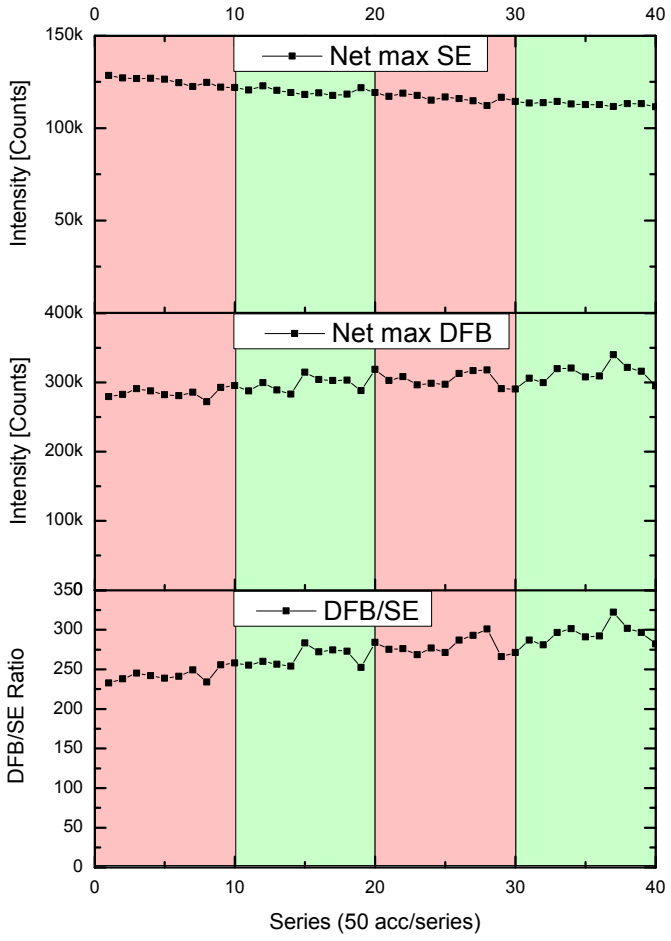


Fig. 15. DFB peak, stimulated emission continuum and ratio of the two parameters (used to normalize DFB peak value in case of input beam intensity drop) of an UGAB sample 25 MBq $^{90}Sr/^{90}Y$ radioactive source.

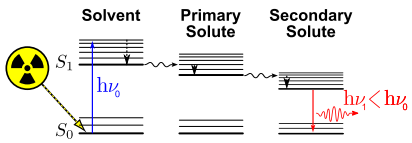


Fig. 16. Typical energy transfer in absorption/emission spectra in a ternary scintillator cocktail.

scintillator, energy deposited by the ionizing radiation excites the solvent and is then transfered through a cascade energy process, leading to the emission by the ternary solute. The excitation of the intermediate solutes by the laser beam might result in a change in the cascade process, thus not impacting the laser emission.

To validate our hypothesis, experiments will involve scintillators in which transfer processes are well understood, *e.g.* binary scintillators with the solvent and only one solute.

Various MCNP simulations are also currently prepared to evaluate and compare more precisely the amount of energy deposited by beta particles in different samples.

## VI. Conclusion

Laser emission has been demonstrated in scintillators using transient gratings.

Most of the results presented herein were obtained using *commercial* liquid scintillators, which are not initially designed for laser applications. Nanostructuration of solid films is sill being investigated.

The results of our preliminary investigation show *promising features* for the future of scintillating detectors.

Undergoing investigations include MCNPX simulations and experimental study of binary scintillators to further understand energy transfer in scintillating cocktails. Other commercial liquid scintillators will soon be characterized as concerns their lasing ability.

## References

[1] M. Gersborg-Hansen and A. Kristensen, "Optofluidic third order distributed feedback dye laser," *Applied Physics Letters*, vol. 89, no. 10, p. 103518, 2006.

[2] P. Coll, M. Cabane, P. Mahaffy, and W. Brinckerhoff, "Sample Analysis at Mars," in *35th COSPAR Scientific Assembly*, vol. 35, 2004, p. 3605.

[3] W. Zeller, L. Naehle, P. Fuchs, F. Gerschuetz, L. Hildebrandt, and J. Koeth, "DFB Lasers Between 760 nm and 16 micrometer for Sensing Applications," *Sensors*, vol. 10, no. 4, pp. 2492–2510, 2010.

[4] A. Rose, Z. Zhu, C. F. Madigan, T. M. Swager, and V. Bulovic, "Sensitivity gains in chemosensing by lasing action in organic polymers," *Nature*, vol. 434, no. 7035, pp. 876–879, Apr 2005.

[5] A. Einstein, "Zur Quantentheorie der Strahlung," *Physikalische Zeitschrift*, vol. 18, pp. 121–128, 1917.

[6] Y. Xia and G. M. Whitesides, "Soft lithography," *Annual Review of Materials Science*, vol. 28, no. 1, pp. 153–184, 1998.

[7] H. Kogelnik and C. V. Shank, "Stimulated emission in a periodic structure," *Applied Physics Letters*, vol. 18, no. 4, pp. 152–155, February 1971.

[8] G. Boulon, "Génération d'impulsions lasers ultracourtes jusquà la femtoseconde," *Techniques de l'ingénieur.*, vol. AF3282, pp. 1–24, 2006.

[9] Eljen. (2013) Plastic Scintillators. Last accessed: June 5th, 2013.

[10] I. D. W. Samuel, E. B. Namdas, and G. A. Turnbull, "How to recognize lasing," *Nat Photon*, vol. 3, no. 10, pp. 546–549, Oct 2009.

[11] Perkin Elmer, *UltimaGold AB Material Safety Datasheet*, 2009.

[12] M. Hamel, S. Normand, A.-M. Frelin, and V. Simic, "Novel 1,8 Naphthalimides for Fast Neutron/Gamma Discrimination in Liquid Scintillators," in *The International Conference on Advances in Liquid Scintillation Spectrometry*, J. Eikenberg, M. Jggi, H. Beer, and H. Baehrle, Eds. Davos, Switzerland: Liquid Scintillation Counting International, May 2008.

[13] H. Kogelnik and C. V. Shank, "Coupled Wave Theory of Distributed Feedback Lasers," *Journal of Applied Physics*, vol. 43, no. 5, pp. 2327 –2335, May 1972.